Texture and Microstructure for Magnetic Properties of Two-Stage Cold-Rolled Fe-6.5 Wt Pct Si Thin Sheets

YONGCHUANG YAO, YUHUI SHA, JINLONG LIU, FANG ZHANG, and LIANG ZUO

Decreasing thickness and optimizing texture are the two critical means to improve the magnetic properties of high-silicon electrical steel sheet. In the present study, the 0.15-mm-thick Fe-6.5 wt pct Si thin sheets were produced by two-stage cold rolling process with intermediate annealing. The effects of intermediate microstructure on recrystallization texture were investigated using X-ray diffraction and electron backscattered diffraction. As the intermediate grain size increases from 40 to 80 μm, the favorable η fiber ($\langle 001\rangle$//RD, rolling direction) is enhanced and harmful γ fiber ($\langle 111\rangle$//ND, normal direction) is weakened after final annealing, and consequently, the magnetic properties are improved evidently. The number and nature of shear bands relative to the grain boundary regions, which are closely related to the intermediate grain size and rolling parameters, are responsible for the recrystallization texture development.

DOI: 10.1007/s11661-015-3057-3

I. INTRODUCTION

HIGH-SILICON electrical steel containing 6.5 wt pct Si has excellent soft magnetic properties such as high permeability, low iron loss, and reduced noise.[1] Owing to the serious brittleness, it is hard to produce Fe-6.5 wt pct Si sheets through the conventional rolling procedure. Several special processing methods such as chemical vapor deposition (CVD),[2] rapid solidification,[3] and spray forming[4] have attracted more attention. However, continuous efforts have also been made on the rolling process, showing that Fe-6.5 wt pct Si thin sheets can be produced successfully by the precise control of hot band microstructure and careful selection of the rolling parameters.[5–8] Because of the high flow stress, it is basically inevitable to apply two-stage cold rolling process with intermediate annealing to fabricate Fe-6.5 wt pct Si thin sheets.

Recrystallization texture is a key factor to improve the magnetic properties in spite of a lower magnetic anisotropy for Fe-6.5 wt pct Si alloy than that for the conventional silicon steel. Recrystallization η fiber ($\langle 001\rangle$//RD, rolling direction) and λ fiber ($\langle 001\rangle$//ND, normal direction) are favorable to magnetic properties with $\langle 001\rangle$ easy magnetization direction lying in the rolling plane, whereas γ fiber ($\langle 111\rangle$//ND) is detrimental without $\langle 001\rangle$ direction in the rolling plane. Limited work has been done on the texture development in Fe-6.5 wt pct Si sheets. Liu *et al.*[7,8] obtained $\{001\}\langle 210\rangle$ and $\{210\}\langle 001\rangle$ recrystallization textures in 0.5-mm-thick rolled Fe-6.5 wt pct Si sheets. Fang *et al.*[9] reported recrystallization η and γ fibers in 0.3-mm-thick rolled 6.5 wt pct Si sheets. Liu *et al.*[10,11] produced recrystallization λ fiber in Fe-6.5 wt pct Si thin sheets by twin-roll strip casting process followed by hot rolling and warm rolling.

Recrystallized η and γ grains mainly nucleate at shear bands and grain boundary regions, respectively.[12–18] In two-stage cold rolling process, intermediate grain size acts as the initial grain size for second-stage rolling. The coarse initial grain size prior to final cold rolling process promotes the formation of shear bands and reduces the grain boundary regions. A number of investigations have revealed that the primary recrystallization η fiber can be enhanced by increasing the initial grain size.[19–24] Nevertheless, it is hard to ignore the fact that recrystallized η grains tend to exist in colonies during recrystallization process and are less favorable in terms of size, whereas γ grains can gain number and size advantages during primary recrystallization in electrical steel and ultra-low carbon steel,[12,25–27] even in the sheets with coarse initial grain size.[21,23] Therefore, it is potentially difficult to enhance η fiber and reduce γ fiber when considerable grain growth is necessary to reach an optimal final grain size. In our previous work, the dominant recrystallization η fiber was achieved after high-temperature annealing by the designed cold rolling parameters in a two-stage rolling process under a fixed intermediate grain size.[28] It is necessary to further explore how the intermediate grain size affects the localized deformation microstructure and nucleation behavior, and how it affects the growth of recrystallized η grains during primary recrystallization and subsequent grain growth process in the Fe-6.5 wt pct Si thin sheets.

In this work, the 0.15-mm-thick Fe-6.5 wt pct Si sheets were produced by two-stage cold rolling. The

YONGCHUANG YAO, Doctoral Student, YUHUI SHA and LIANG ZUO, Professors, JINLONG LIU, Lecturer, and FANG ZHANG, Associate Professor, are with the Key Laboratory for Anisotropy and Texture of Materials (Ministry of Education), Northeastern University, Shenyang 110819, P.R. China. Contact e-mail: yhsha@mail.neu.edu.cn

Manuscript submitted January 31, 2015.
Article published online July 18, 2015

development of microstructure and texture with different intermediate grain sizes was investigated to enrich the routines for improving recrystallization texture and magnetic properties.

II. EXPERIMENTAL PROCEDURE

Fe-6.5 wt pct Si ingots were prepared in a vacuum induction furnace and homogenized in 1473 K (1200 °C) for 30 minutes. The ingots were first forged into 60-mm-thick slabs, then reheated at 1473 K (1200 °C) for 30 minutes, and continuously hot rolled to 1.75 mm. The hot bands were normalized at 1423 K (1150 °C) for 5 minutes, then the normalized bands were first cold rolled to 0.5 mm with the reduction of 72 pct, then an intermediate annealing was performed at 1098 K (825 °C) for 5 minutes, 1223 K (950 °C) for 10 minutes, and 1373 K (1100 °C) for 5 minutes to obtain the intermediate grain sizes of 40, 80, and 120 μm, respectively. Nearly all the recrystallized grains after intermediate annealing are equiaxed, and the intermediate grain size was measured by mean interception length method. Afterward, the annealed sheets were further cold rolled to 0.15 mm with 70 pct reduction. The two stages of cold rolling were both carried out with the rolling speed of 6 m/min at 473 K (200 °C). Final annealing process was conducted as follows: samples were pushed in tube furnace at 973 K (700 °C), then the temperature was continuously raised to 1423 K (1150 °C) with a heating rate of 20 K/h (20 °C/h) under argon atmosphere.

For pole figure measurements, the samples were first mechanically polished and then electropolished in a solution of 80 pct ethanol and 20 pct perchloric acid. Orientation distribution functions (ODFs) of the rolled and annealed sheets were measured at quarter layer using X'Pert PRO diffractometer with a radiation source of Co K_α. Electron backscattered diffraction (EBSD) was performed to analyze the formation of recrystallization texture. The magnetic flux density at field strength of 800 A/m (B_8) and the iron loss at 1.0 tesla and 50 Hz ($P_{10/50}$) were measured by IWATSU SY-8232 B-H analyzer.

III. RESULTS

Figure 1 presents the microstructure and texture of cold-rolled Fe-6.5 wt pct Si sheets with different intermediate grain sizes. A prominent microstructure difference can be observed that shear bands are widely distributed in most of the deformed grains for the specimen with coarse intermediate grain size (hereafter defined as coarse-grained specimen), while shear banding only occurs locally for the specimen with fine intermediate grain size (hereafter defined as fine-grained specimen). Moreover, shear bands in fine-grained specimen are much shorter due to the limited grain boundary spacing along sheet thickness. The texture of the fine-grained specimen has a strong complete γ fiber and a partial α fiber ($\langle 110\rangle$//RD), which is similar to the observed rolling textures in

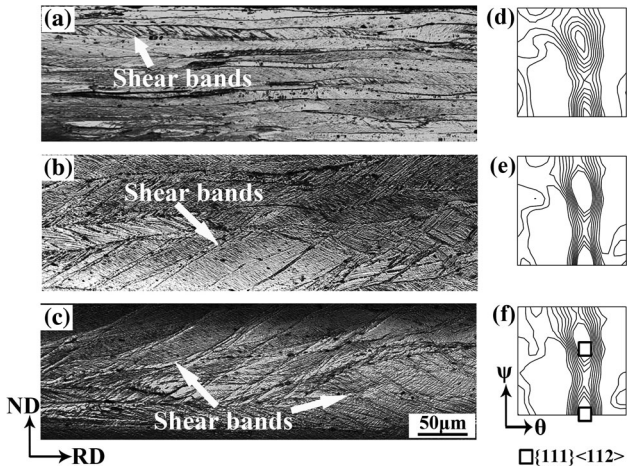

Fig. 1—Microstructure of Fe-6.5 wt pct Si thin sheets after second-stage cold rolling with intermediate grain sizes of (*a*) 40, (*b*) 80, and (*c*) 120 μm. Constant $\varphi = 45$ deg sections of ODFs of Fe-6.5 wt pct Si thin sheets after second-stage cold rolling with intermediate grain sizes of (*d*) 40, (*e*) 80, and (*f*) 120 μm (magnification: ×1).

electrical and ultra-low carbon steel.[12,19,29] However, the texture in coarse-grained specimen has a much strong $\{111\}\langle 112\rangle$ component and fairly weak minor components, such as $\{001\}\langle 110\rangle$ and $\{112\}\langle 110\rangle$. Park *et al.*[23] reported similar results concerning the cold rolling texture of different initial grain sizes.

Both grain boundaries and shear bands are high stored energy regions and preferential nucleation sites during recrystallization process. The change in the number and morphology of shear bands will affect the development of recrystallization η and γ fibers. Figure 2 illustrates the orientation image maps at the early stage of recrystallization. It can be clearly seen that the intermediate grain size has obvious effects on nucleation features: in fine-grained specimen, recrystallized η and γ grains are tangled together and the location of original shear bands can hardly be discerned; by contrast, in coarse-grained specimen, a number of η grains are nucleated along shear bands and surrounded with wide deformed matrix.

Figure 3 gives the constant $\varphi = 0$ and 45 deg sections of the ODFs after final annealing. The recrystallization texture mainly consists of η and γ fibers for both fine- and coarse-grained specimens; however, η fiber with peak at $\{210\}\langle 001\rangle$ is enhanced and γ fiber is significantly weakened with the increase of intermediate grain size. Although the intensity of η fiber exhibits slight decrease as the intermediate grain size further increases from 80 to 120 μm, the intensity of γ fiber is continuously reduced with the increase of intermediate grain size.

The final grain size and magnetic properties of B_8 and $P_{10/50}$ are shown in Figure 4. The final grain size increases sharply as the intermediate grain size changes from 40 to 80 μm, while only a slight increase occurs with further increase of intermediate grain size. Magnetic properties exhibit a more sensitive dependence that, in the case of coarse-grained specimen, the increased magnetic induction (B_8) is attributed to the improved recrystallization texture, while the evidently

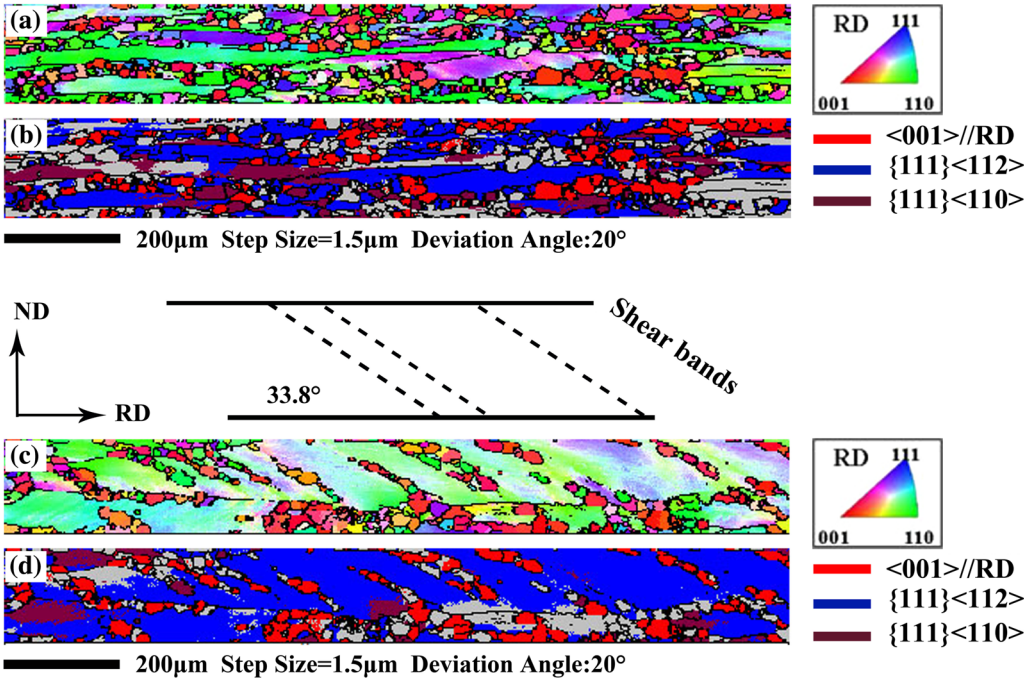

Fig. 2—(*a*) Orientation image maps of all orientations and (*b*) several main components of the partially recrystallized state in Fe-6.5 wt pct Si thin sheets after second-stage cold rolling with intermediate grain size of 40 μm. (*c*) Orientation image maps of all orientations and (*d*) several main components of the partially recrystallized state in Fe-6.5 wt pct Si thin sheets after second-stage cold rolling with intermediate grain size of 120 μm (magnification: ×1).

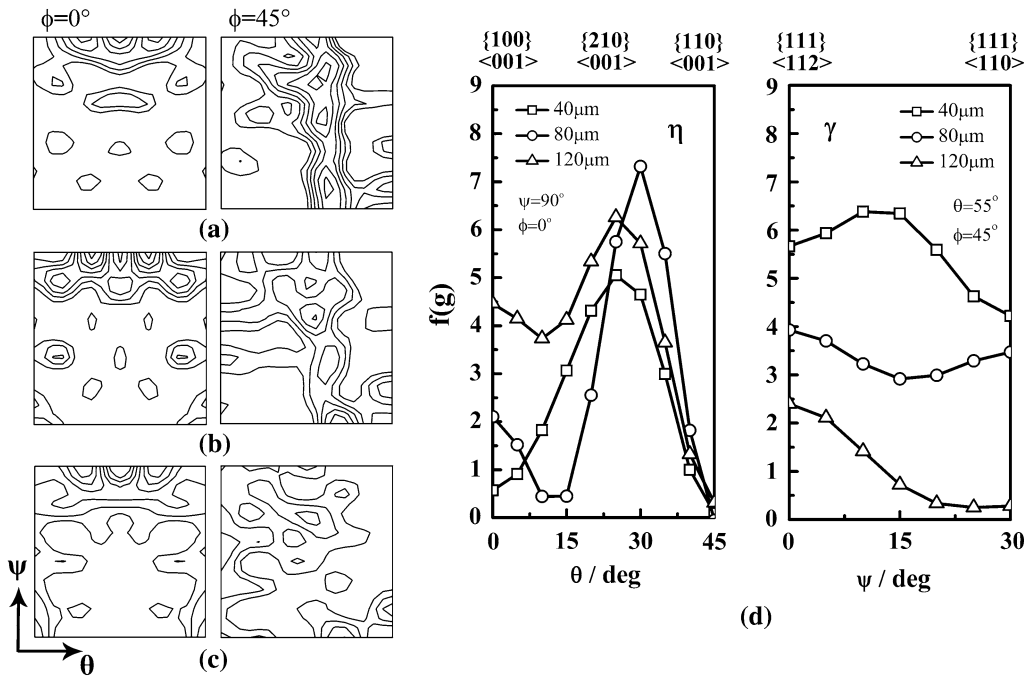

Fig. 3—Constant φ = 0 and 45 deg sections of the ODFs of Fe-6.5 wt pct Si thin sheets after final annealing, corresponding to intermediate grain sizes: (*a*) 40, (*b*) 80, and (*c*) 120 μm. (*d*) Orientation densities along η and γ fibers after final annealing corresponding to different intermediate grain sizes (magnification: ×1).

reduced iron loss is attributed to the combined contribution from final grain size and recrystallization texture.[30] Moreover, the magnetic induction for the 120 μm intermediate grain size is slightly lower than that for the 80 μm intermediate grain size, which is reasonably related with the slight decrease of η fiber.

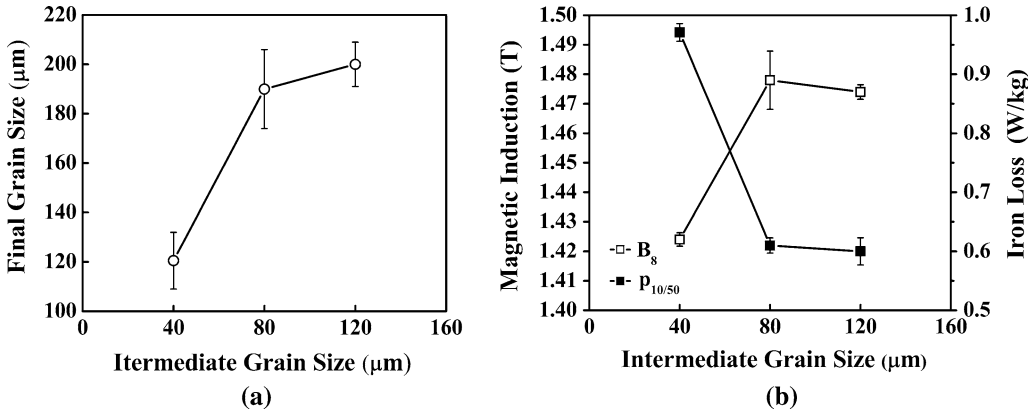

Fig. 4—(*a*) The grain size and (*b*) magnetic properties of B_8, $P_{10/50}$ of Fe-6.5 wt pct Si thin sheets after final annealing (magnification: ×1).

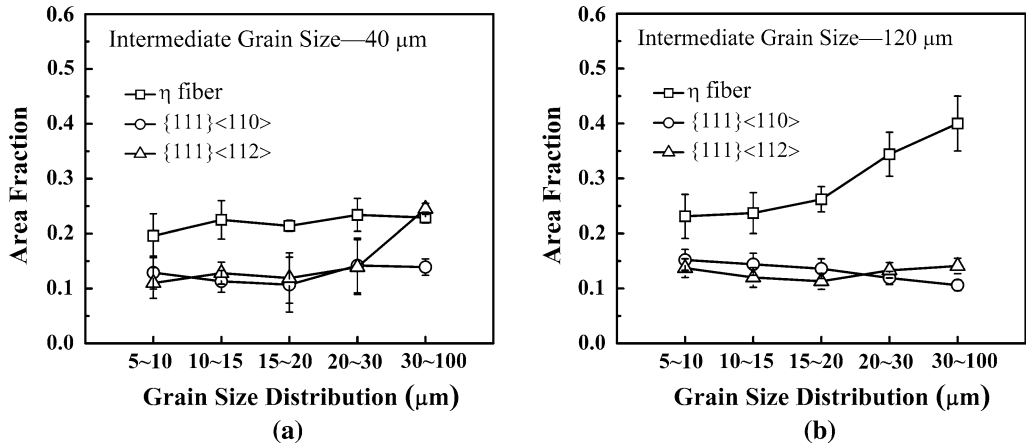

Fig. 5—Area fraction distribution of main texture components in just fully recrystallized state obtained from EBSD in Fe-6.5 wt pct Si thin sheets with intermediate grain sizes of (*a*) 40 and (*b*) 120 μm (magnification: ×1).

IV. DISCUSSION

In coarse-grained specimen, recrystallization η fiber becomes the dominant texture component and γ fiber has been largely reduced after considerable grain growth in the present work. This is in contrast to the observation in coarse-grained specimen that η fiber tends to weaken during further grain growth because of similar orientation among the clustered η grains along shear bands.[21,23]

Figure 5 gives the area fraction distribution of main texture components in a series of grain size intervals in just fully recrystallized sample. For each grain size interval, the ratio between the area of one texture component and the total area of the grain size interval represents the area fraction of the specific component in this grain size bin. There are at least 180 grains included for one texture component in each grain size bin to ensure a statistical significance. In the case of fine-grained specimen, η grains have an advantage in area fraction over various grain size intervals except for the large grain size interval, showing that η grains have no size advantage valuable for grain growth stage. However, in the case of coarse-grained specimen, η grains occupy nearly 40 pct of the area among grains between 30 and 100 μm, indicating the obvious size advantage of η grains, which is different from the general understanding that η grains have no size advantage during primary recrystallization.[12,25,26]

The lack of size advantage for recrystallized η grains may be attributed to their dense nucleation sites at the shear bands. The excessively high stored energy within shear bands can cause a high nucleation rate and a large number of η grains are clustered; this means that η grains form colonies and have a similar orientation to each other,[23,25,26] those clustered η grains are normally smaller in size and have a much higher possibility of being surrounded by low-angle grain boundaries, and the growth rate of η grains must be low.[23,26] Therefore, the appropriate density and intensity of shear bands are important for η grains to gain number and size advantages in primary recrystallization.

In the present work, the coarse intermediate grain size promotes the formation of shear bands in most of the deformed grains. Moreover, cold rolling at 473 K (200 °C) allows to avoid the rapid accumulation of strain stored energy within shear bands, thus meliorates

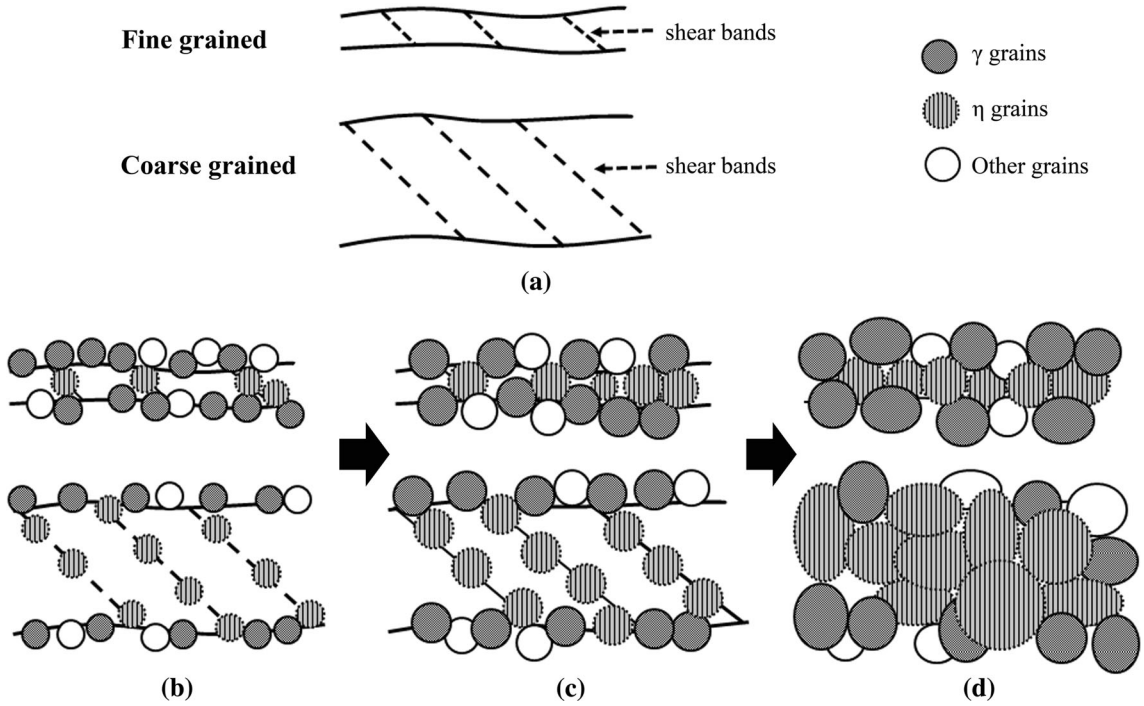

Fig. 6—Schematic representation of the nucleation of η and γ grains during primary recrystallization. (*a*) Shear bands in cold-rolled matrix, (*b*) η and γ grains nucleated in shear bands at early stage of recrystallization, (*c*) the growth of η and γ grains, and (*d*) complete recrystallization (magnification: ×1).

the severity of clustering and increases the nucleation size of η grains. Liu *et al.*[8] and Yao *et al.*[28] also reported the role of cold rolling at 473 K (200 °C) on the moderate intensity and density of shear bands in rolled Fe-6.5 wt pct Si sheets.

Based on the above analysis, a mechanism regarding the effects of initial grain size prior to final rolling is proposed to explain the competition between η and γ grains during primary recrystallization (Figure 6). For fine-grained specimens, η grains nucleated at short shear bands will come in contact quickly with other grains nucleated at the grain boundary regions. This implies that η grains have no enough time and space to grow before complete recrystallization. On the contrary, in coarse-grained specimens, shear bands can provide plentiful nucleation sites for η grains and wide deformed matrix around these η grains. The appropriate stored energy in shear bands can avoid dense clustering of η grains, and the longer shear bands can ensure a large distance between new η and γ grains. Thus, η grains have adequate time and space to grow before coming into contact with γ grains. Consequently, in the case of coarse intermediate grain size together with appropriate rolling process, η grains can gain both number and size advantages in primarily recrystallized microstructure, producing the dominant η fiber after considerable grain growth. However, an excessively coarse intermediate grain size can also evidently expand the growth space for γ grains, leading to a possible reduction of η fiber.

V. CONCLUSIONS

Fe-6.5 wt pct Si thin sheets were produced by two-stage cold rolling with intermediate annealing. The improved recrystallization texture characterized with enhanced η fiber and significantly weakened γ fiber is obtained in the case of coarse intermediate grain size after high-temperature annealing. The proper density and intensity of shear bands as well as reduced grain boundary area are the critical factors for η grains to obtain both number and size advantages in the primary recrystallization stage, which makes η fiber become the dominant texture component after grain growth.

ACKNOWLEDGMENTS

This work is supported by the National High Technology Research and Development Program of China (Grant No. 2012AA03A505), as well as the National Natural Science Foundation of China (51171042, 51101031), and the Specialized Research Fund for the Doctoral Program of Higher Education (20110042110002).

REFERENCES

1. M. Abe, Y. Takada, T. Murakami, Y. Tanaka, and Y. Mihara: *J. Mater. Eng.*, 1989, vol. 11, pp. 109–16.

2. T. Yamaji, M. Abe, Y. Takada, K. Okada, and T. Hiratani: *J. Magn. Magn. Mater.*, 1994, vol. 133, pp. 187–89.
3. M. Baricco, E. Mastrandrea, C. Antonione, B. Viala, J. Degauque, E. Ferrara, and F. Fiorillo: *Mater. Sci. Eng.*, 1997, vols. A226–228, pp. 1025–29.
4. A.H. Kasama, C. Bolfarini, C.S. Kiminami, and W.J. BottaFilho: *Mater. Sci. Eng.*, 2007, vols. A449–451, pp. 375–77.
5. Y. Takada, M. Abe, S. Masuda, and J. Inagaki: *J. Appl. Phys.*, 1988, vol. 64 (10), pp. 5367–69.
6. T. Ros, Y. Houbaert, O. Fischer, and J. Schneider: *J. Mater. Process. Technol.*, 2003, vol. 141, pp. 132–37.
7. J.L. Liu, Y.H. Sha, F. Zhang, H.P. Yang, and L. Zuo: *J. Appl. Phys.*, 2011, vol. 109, pp. 1–3.
8. J.L. Liu, Y.H. Sha, F. Zhang, J.C. Li, Y.C. Yao, and L. Zuo: *Scripta Mater.*, 2011, vol. 65 (4), pp. 292–95.
9. X.S. Fang, Y.F. Liang, F. Ye, and J.P. Lin: *J. Appl. Phys.*, 2012, vol. 111, pp. 1–4.
10. H.T. Liu, Z.Y. Liu, Y. Sun, F. Gao, and G.D. Wang: *Mater. Lett.*, 2013, vol. 91, pp. 150–53.
11. H.Z. Liu, H.T. Liu, Z.Y. Liu, H.H. Lu, H.Y. Song, and G.D. Wang: *Mater. Charact.*, 2014, vol. 88, pp. 1–6.
12. J.T. Park and J.A. Szpunar: *Acta Mater.*, 2003, vol. 51, pp. 3037–51.
13. K. Murakami, N. Morishige, and K. Ushioda: *Mater. Sci. Forum*, 2012, vols. 715–716, pp. 158–63.
14. Y.H. Sha, C. Sun, F. Zhang, D. Patel, X. Chen, S.R. Kalidindi, and L. Zuo: *Acta Mater.*, 2014, vol. 76, pp. 106–17.
15. Y. Wang, Y.B. Xu, Y.X. Zhang, F. Fang, X. Lu, H.T. Liu, and G.D. Wang: *J. Magn. Magn. Mater.*, 2015, vol. 379, pp. 161–66.
16. M.R. Barnett and L. Kestens: *ISIJ Int.*, 1999, vol. 39 (9), pp. 923–29.
17. Y.Y. Tse, G.L. Liu, and B.J. Duggan: *Scripta Mater.*, 2000, vol. 42, pp. 25–30.
18. M.Z. Quadir and B.J. Duggan: *Acta Mater.*, 2006, vol. 54, pp. 4337–50.
19. R.K. Ray, J.J. Jonas, and R.E. Hook: *Int. Mater. Rev.*, 1994, vol. 39, pp. 129–72.
20. M.F. de Campos, F.J.G. Landgraf, R. Takanohashi, F.C. Chagas, I.G.S. Falleiros, G.C. Fronzaglia, and H. Kahn: *ISIJ Int.*, 2004, vol. 44 (3), pp. 591–97.
21. S. da Costa Paolinelli, M.A. da Cunha, and A.B. Cota: *J. Magn. Magn. Mater.*, 2008, vol. 320, pp. e641–44.
22. R.F. de Araujo Cardoso, L. Brandao, and M.A. da Cunha: *J. Mater. Res.*, 2008, vol. 11 (1), pp. 51–55.
23. J.T. Park and J.A. Szpunar: *J. Magn. Magn. Mater.*, 2009, vol. 321, pp. 1928–32.
24. S.S.F. de Dafé, S. da Costa Paolinelli, and A.B. Cota: *J. Magn. Magn. Mater.*, 2011, vol. 323, pp. 3234–38.
25. I. Samajdar, S. Cicale, B. Verlinden, P. Van Houtte, and G. Abbruzzesse: *Scripta Mater.*, 1998, vol. 39 (8), pp. 1083–88.
26. J.T. Park and J.A. Szpunar: *ISIJ Int.*, 2005, vol. 45, pp. 743–49.
27. J.L. Bocos, E. Novillo, M.M. Petite, A. Iza-Mendia, and I. Gutierrez: *Metall. Mater. Trans. A*, 2003, vol. 34A, pp. 827–39.
28. Y.C. Yao, Y.H. Sha, J.L. Liu, F. Zhang, and L. Zuo: *J. Electron. Mater.*, 2014, vol. 43 (1), pp. 121–25.
29. K. Verbeken, L. Kestens, and J.J. Jonas: *Scripta Mater.*, 2003, vol. 48, pp. 1457–62.
30. K.M. Lee, S.Y. Park, M.Y. Huh, J.S. Kim, and O. Engler: *J. Magn. Magn. Mater.*, 2014, vol. 354, pp. 324–32.